ROMANIAN JOURNAL OF INFORMATION SCIENCE AND TECHNOLOGY
Volume **10**, Number 2, 2007, 167–176

Vector Discretization Schemes in Technology CAD Environments

O. TRIEBL, T. GRASSER

Christian Doppler Laboratory for TCAD in Microelectronics
at the Institute for Microelectronics, TU Wien
Gußhausstraße 27–29/E360, A-1040 Wien, Austria
E-mail: {Triebl|Grasser}@iue.tuwien.ac.at

Abstract. In Technology CAD (TCAD) environments, a proper vector discretization in two or three dimensions is of crucial importance because physical models used in semiconductor device simulation tools depend on vector quantities. We discuss two discretization methods for Delaunay meshes that are based on the unstructured neighborhood information. In addition a comparison to an element based method is given. Overall good convergence is achieved by applying these methods in a TCAD environment for the calculation of the driving force, electric field, and the current density vector. An example simulation of a diode in breakdown and a bipolar structure in snap-back operation is presented.

1. Introduction

Simulation environments for semiconductor devices, usually known as Technology CAD (TCAD) tools, model the device physics using basic semiconductor equation sets, consisting of partial differential equations (PDE). Because of the complexity of the PDEs in non trivial semiconductor devices, analytical solutions are usually not available and numerical methods have to be applied [1]. Consequently, discretization in time and space is necessary, where the latter is discussed in this paper.

Different transport models can be used for device simulation, the drift-diffusion model, the hydrodynamic model and the six-moments method are three examples. For demonstration purposes the drift-diffusion transport model, consisting of Poisson's equation and the current density relation is selected in this paper. There are three independent variables, the electrostatic potential (Ψ) and the electron and hole concentrations (n and p). The discretization of the equations is commonly done using the box integration method [2]. The basic transformation used within the box

integration method concerns the divergence operator. Applying an integration over a volume V_i and using Gauss' theorem on the basic equation $\nabla \cdot \mathbf{F} = G$ leads to

$$\sum_{\text{all neighbors } j} F_{ij} A_{ij} = G_i V_i \,. \tag{1}$$

This formulation describes fluxes F_{ij} leaving a Voronoi box i to a neighboring box j along a connecting edge d_{ij} via the surface area A_{ij} (see Fig. 1). With the summation of all those weighted fluxes and by using a generation term (G_i) inside the box volume V_i, scalar quantities in each box i can be approximated with a description similar to (1). For the calculation of this discretization, the only geometric information necessary is the unstructured neighborhood information. This includes a list of all mesh points with their associated volumes, together with a connectivity list with one entry for each connection that contains the associated distances d_{ij} and the areas A_{ij}. This formulation is very flexible and also independent of the problem dimension.

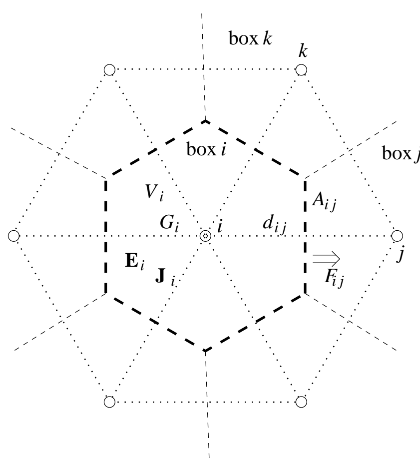

Fig. 1. Voronoi box i of mesh point i with connections to neighboring mesh points. The flux from box i to box j (F_{ij}) through the area A_{ij} is depicted. The vector quantities $\mathbf{E}_i$ and $\mathbf{J}_i$ are constant over the whole box i.

Fluxes are defined along an edge d_{ij} and represent the projection of a vector quantity on the edge: $F_{ij} = \mathbf{e}_{ij} \cdot \mathbf{F}$, with $\mathbf{e}_{ij}$ being the unit vector pointing from mesh point i to mesh point j. In the drift-diffusion model two types of fluxes are used, the dielectric flux and the electron and hole current. The dielectric flux is approximated using finite differences and the current density using the Scharfetter-Gummel discretization [3].

The system of the PDEs is commonly solved with an iterative Newton solver. The solution variables, i.e. Ψ, n and p, are quantities defined at the mesh points and are known after each Newton iteration step. The fluxes from one box to a neighboring box can be calculated using these results. There are physical models, like the carrier mobility $\mu(\mathbf{F})$ or the impact ionization rate $G_{II}(\mathbf{J}, \mathbf{F})$, that depend

on vector quantities, in this case the driving force **F** and the current density **J**. It is therefore necessary to have a representation of vector quantities within the area of the box. Since the results form those models influence the solution variables, the vector discretization has a considerable impact on the simulation result as well as on the convergence behavior of the Newton solver. To achieve convergence, derivatives of the vector quantities are needed to calculated the Jacobian matrix, especially when one of the named models dominates the device behavior.

Laux proposed a method to determine the impact ionization generation rate on triangular meshes [4]. The electric field is evaluated inside one triangle by a linear interpolation of the electrostatic potential ($\mathbf{E} = \mathbf{E}(\Psi_i, \Psi_j, \Psi_k, \text{geometry})$). In contrast, the current density that is calculated with the non linear Scharfetter-Gummel discretization, is evaluated individually for three different regions (see $\mathbf{J}_1, \mathbf{J}_2, \mathbf{J}_3$ in Fig. 2), by using a weighted linear combination of the current densities along the edges: $\mathbf{J}_\nu = \mathbf{J}_\nu(J_{ij}, J_{jk}, J_{ki}, \text{geometry})$, $\nu \in \{1, 2, 3\}$, so there are three different rates calculated for each element. The element based calculation of the vector quantities requires information about triangles (in 2D) or tetrahedrons (in 3D) within the implementation of this scheme and have to be stored in addition to the unstructured neighborhood information. Furthermore, a different implementation for two- and three-dimensional meshes is required.

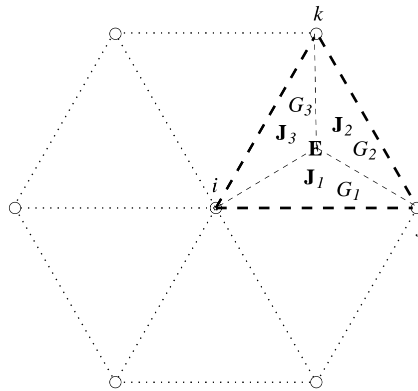

Fig. 2. Approach by S. Laux [4]: The electric field **E** is constant within one triangle and each triangle has one current density vector $\mathbf{J}_x$ for each edge.

In this work, two approaches are presented that assume all vector quantities constant over one Voronoi box, consistent with the box integration method, that only depend on the unstructured neighborhood information. Only quantities from the boxes i and j are needed for evaluating the flux F_{ij}. Both presented approaches aim to meet the following demands:

- simple coupling with box integration method
- exact solution for homogenous fields

- numerical stability

After the derivation, a short discussion of the two approaches is given and example simulations will be presented.

2. Derivation of vector discretization schemes

Two possible derivations for vector discretizations will be given in the following. The derivations are shown for the electric field, the generalization to gradient based fluxes is straight forward.

A. Scheme A

The first discretization scheme defines the projected component E^α in the direction $\mathbf{e}_\alpha$ from the electric field $\mathbf{E}$, where Ψ is the electrostatic potential:

$$E^\alpha = \mathbf{e}_\alpha \cdot \mathbf{E} = -\mathbf{e}_\alpha \cdot \nabla \left(\Psi - \Psi_i\right) \tag{2}$$

By integration over the box volume V and by applying Gauss' theorem, (2) evaluates to

$$\int E^\alpha \mathrm{d}V = -\oint \big(\Psi - \Psi_i\big) \mathbf{e}_\alpha \mathrm{d}\mathbf{A}\,. \tag{3}$$

By approximating the integral with a sum, E_i^α in box i can be written as

$$E_i^\alpha = \frac{1}{V_i} \sum_j A_{ij} \frac{\Psi_i - \Psi_j}{2} \mathbf{e}_\alpha \cdot \mathbf{e}_{ij}\,, \tag{4}$$

where the sum includes all neighbors j, A_{ij} is the surface between the two boxes i and j and Ψ_ν is the electrostatic potential in mesh point ν. By defining $\mathbf{E}_i = (E_i^x\ E_i^y)^\mathrm{T}$, $\mathbf{E}_i$ can be written as

$$\mathbf{E}_i = \frac{1}{2V_i} \sum_j A_{ij} \mathbf{d}_{ij} E_{ij}, \tag{5}$$

where $d_{ij} = |\mathbf{d}_{ij}|$ with $\mathbf{d}_{ij} = (x_j - x_i\ \ y_j - y_i)^\mathrm{T}$ and E_{ij} is the component of the electric field at the boundary between box i and j

$$E_{ij} = -\frac{\Psi_j - \Psi_i}{d_{ij}}. \tag{6}$$

B. Scheme B

The second discretization scheme is an extension of the finite difference method and is based on a scheme proposed in [5]. Considering the box 0 in a non-equidistant orthogonal mesh depicted in Fig. 3 and its neighboring box 1 (not shown explicitly), the electric field along the edge d_{01} can be expressed as $E = -\mathrm{d}\Psi/\mathrm{d}x$. At the

boundary between the two boxes, i.e. the midpoint between 0 and 1, the finite difference method gives

$$E_{01} = -\frac{\Psi_1 - \Psi_0}{d_{01}}\,, \tag{7}$$

the same result as in (6). The electric field E_0^x in direction $\mathbf{e}_x$ at mesh point 0 is expressed with a linear interpolation (8), the same procedure is applied to the component E_0^y (9).

$$E_0^x = \frac{\dfrac{E_{01}}{x_1 - x_0} + \dfrac{E_{02}}{x_2 - x_0}}{\dfrac{1}{x_1 - x_0} + \dfrac{1}{x_2 - x_0}} \tag{8}$$

$$E_0^y = \frac{\dfrac{E_{03}}{y_3 - y_0} + \dfrac{E_{04}}{y_4 - y_0}}{\dfrac{1}{y_3 - y_0} + \dfrac{1}{y_4 - y_0}} \tag{9}$$

An extension of this equation set, that also allows edges not aligned with the coordinate axis is

$$\begin{aligned}\frac{1}{x_j - x_i} &\Rightarrow \frac{x_j - x_i}{(x_j - x_i)^2 + (y_j - y_i)^2} \\ &= \frac{x_j - x_i}{d_{ij}^2}\,.\end{aligned} \tag{10}$$

With the already specified vector $\mathbf{E}_i$ and with $\mathbf{e}_{ij} = \mathbf{d}_{ij}/d_{ij}$, a closed vector representation can be given, where the area A_{ij} is used as a weighting factor.

$$\underbrace{\sum_j \frac{A_{ij}}{d_{ij}} \left(\mathbf{e}_{ij} \otimes \mathbf{e}_{ij}\right)}_{\mathbb{M}_i} \mathbf{E}_i = \sum_j \frac{A_{ij}}{d_{ij}} \mathbf{e}_{ij} E_{ij} \tag{11}$$

Note that (8) and (9) are still retained and can be extracted by using $\mathbf{e}_{ij} = (1\ 0)^{\mathrm{T}}$ and $\mathbf{e}_{ij} = (0\ 1)^{\mathrm{T}}$, respectively. $\mathbf{E}_i$ at the left side of (11) can be taken out of the sum and the remaining part of the sum results in a pure geometry dependent matrix, which is calculated once in the beginning of the simulation. This allows the convenient formulation of the final discretization rule for a vector $\mathbf{E}_i$ in point i (12), using the geometry matrix $\mathbb{M}_i$ (13) and the geometry factor (14).

$$\mathbf{E}_i = \mathbb{M}_i^{-1} \sum_j g_{ij} \mathbf{e}_{ij} E_{ij} \tag{12}$$

$$\mathbb{M}_i = \sum_j g_{ij} \mathbf{e}_{ij} \otimes \mathbf{e}_{ij} \tag{13}$$

$$g_{ij} = \frac{A_{ij}}{d_{ij}} \tag{14}$$

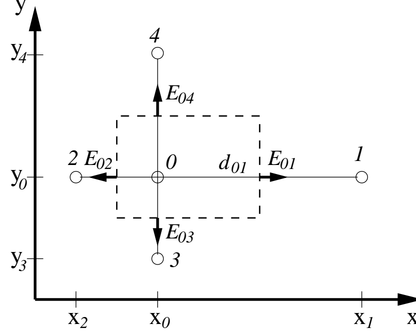

Fig. 3. Voronoi box of mesh point 0 with its neighboring points 1-4 in a non equidistant orthogonal mesh. The contributing field components E_{ij} from the edges are depicted.

3. Properties of the discretization schemes

Both derivations are based on the unstructured neighborhood information only, so they can be easily coupled with the box integration method.

The second demand, the exact solution for a homogenous fields $\mathbf{E} = \mathbf{E}_H$, with the electrostatic potential $\Psi(\mathbf{x}) = -\mathbf{E}_H \cdot \mathbf{x}$, was verified in (15) on scheme A limited on orthogonal grids $\mathrm{d}_{ij}/d_{ij} \in \{(\pm 1\ \ 0)^{\mathrm{T}}, (0\ \pm 1)^{\mathrm{T}}\}$.

$$\mathbf{E}_i = \frac{1}{2V_i} \sum_j g_{ij} \left(\mathbf{d}_{ij} \otimes \mathbf{d}_{ij}\right) \mathbf{E}_H = \mathbf{E}_H \tag{15}$$

For scheme B a general proof was performed:

$$\mathbf{E}_i = \mathbb{M}_i^{-1} \sum_j g_{ij} \left(\mathbf{e}_{ij} \otimes \mathbf{e}_{ij}\right) \mathbf{E}_H = \mathbf{E}_H . \tag{16}$$

The results of the discretization schemes with a linear electric field $E(x) = -2\alpha x$ and an quadratic electrostatic potential $\Psi(x) = \alpha x^2$ was investigated in one dimension. Using only the x-axis and the naming convention from Fig. 3, the discretization scheme A results in (17) and scheme B results in the exact solution (18).

$$E_{\mathrm{A}}(x_0) = -\alpha(x_1 - x_2) \tag{17}$$

$$E_{\mathrm{B}}(x_0) = -2\alpha x_0 \tag{18}$$

The error of scheme A depends on the the ratio d_{01}/d_{02} and results in

$$\epsilon_{\mathrm{A}}(x_0) = \frac{E_{\mathrm{A}}(x_0)}{E(x_0)} = \frac{1}{2}\left(\frac{d_{01}}{d_{02}} + 1\right) . \tag{19}$$

With a mesh distance ratio in the range $[1/1.16 \ldots 1.16]$, the error is bound to 30 %.

The reference point taken as the correct solution in a box is the mesh point itself, scheme B delivers this solution. Scheme A in contrast delivers the solution of the point in the center between the two neighboring points which usually differs from the mesh point. The examples in the next section will show how this difference may effect the simulation result. In future work it has to be determined, if the mesh point itself is a good choice for adequate vector modeling over the whole box, expecially when it is shifted away from the box center. Additionally, investigations for higher dimensions are necessary to find more results and comparison criteria for the two discretization schemes.

Analyzing the geometry matrix $\mathbb{M}_i$ in scheme B shows, that it results from a sum of symmetric matrices $\mathbf{e}_{ij} \otimes \mathbf{e}_{ij}$ whose determinants equal 0 and whose main diagonals are positive. The sum of symmetric matrices with positive main diagonals and non-negative determinants results in a symmetric matrix with positive main diagonal and a non-negative determinant. If at least two of the participating matrices are linear independent, the determinant of the geometry matrix is positive. As long as the Delaunay criterion is fulfilled, there are always linear independent edges for one box and the inverse geometry matrix can be calculated.

The introduction already stated that the derivatives on mesh points are needed for the Jacobian matrix. This makes it necessary, that the derived discretization schemes are also differentiable on quantities ξ_k associated to a mesh point k. This is indeed possible and one obtains for scheme A:

$$\frac{\partial \mathbf{E}_i}{\partial \xi_k} = \frac{1}{2V_i} \sum_j A_{ij} \mathbf{d}_{ij} \frac{\partial E_{ij}}{\partial \xi_k}, \tag{20}$$

and for scheme B:

$$\frac{\partial \mathbf{E}_i}{\partial \xi_k} = \mathbb{M}_i^{-1} \sum_j g_{ij} \mathbf{e}_{ij} \frac{\partial E_{ij}}{\partial \xi_k}. \tag{21}$$

In both discretization schemes, the existence of $\dfrac{\partial E_{ij}}{\partial \xi_k}$, which is available in any device simulation based on the box integration method, is sufficient to calculate $\dfrac{\partial \mathbf{E}_i}{\partial \xi_k}$.

4. Examples

To demonstrate the applicability of these discretization schemes and to show the differences in the results, two 2D simulation examples will be given. Impact ionization was selected as a good example for a physical model that strongly depends on vector quantities and that strongly influences the device behavior. This generation term is one of the most challenging problems in numerical simulation, especially when it is the dominating physical effect. For modeling impact ionization in the drift-diffusion equation set, a modified version of the model [1] has been chosen:

$$G^{\mathrm{II}} = \alpha_n \frac{|\mathbf{J}_n|}{\mathrm{q}} + \alpha_p \frac{|\mathbf{J}_p|}{\mathrm{q}}. \tag{22}$$

G^{II} is the impact ionization generation term added to the right hand side of the continuity equation. $\mathbf{J}_n$ and $\mathbf{J}_p$ are the electron and hole current densities, q is the elementary charge and α_ν, $\nu \in \{n, p\}$, is defined as

$$\alpha_\nu = \alpha_\nu^\infty \exp\left(-\left(\frac{E_\nu^{\mathrm{crit}}}{|\mathbf{F}_\nu|}\right)^{\beta_\nu}\right), \tag{23}$$

where α_ν^∞, E_ν^{crit} and β_ν are material dependent parameters. The difference to the model in [1] is, that the driving force $\mathbf{F}_\nu$ is used instead of the electric field. The simulations were performed with an adapted version of MINIMOS-NT [6], all derivatives of the impact ionization terms were calculated and added to the Jacobian matrix.

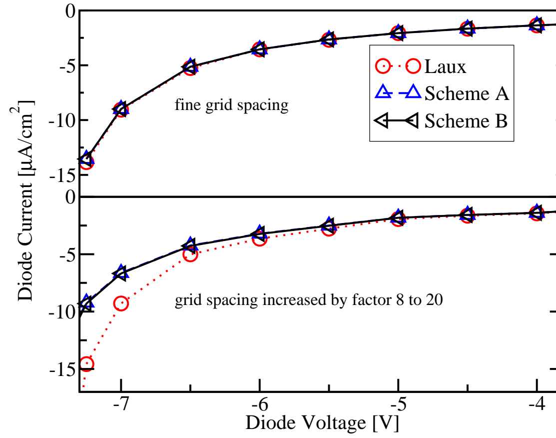

Fig. 4. Simulation of a reverse biased diode using different vector discretization schemes and different meshes.

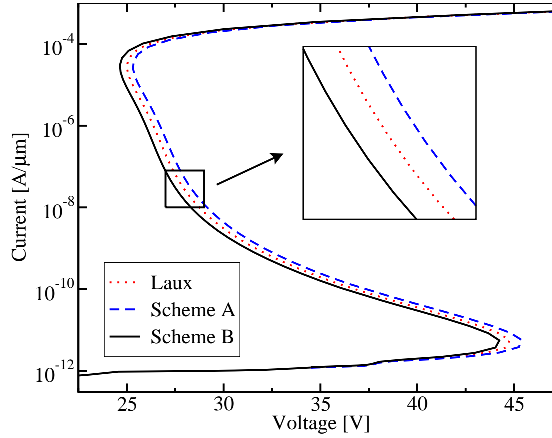

Fig. 5. Simulation of an $\mathrm{n}^+\,\mathrm{p}\,\mathrm{n}\,\mathrm{n}^+$ structure in snap-back using different vector discretization schemes.

The first device that was simulated is a reverse biased diode with an abrupt pn-junction, a donor concentration of 10^{20} 1/cm^2 and an acceptor concentration of 10^{17} 1/cm^2. A comparison of the two presented discretization schemes for unstructured neighborhood information and the scheme from Laux using using two different meshes is shown in Fig. 4. The simulation results on a very fine mesh can be seen in the upper half of the figure. As expected, the results are the same for all three schemes. Increasing the mesh spacing by a factor of 8 near the junction and a factor of 20 near the contacts shows that using scheme A and scheme B give results worse than obtained from the scheme of Laux. In the element based scheme, three different generation rates are calculated for each element, in the two other schemes there is only one rate for the whole Voronoi box. This is comparable to an implicit higher resolution. However, the scheme from Laux requires a more complex calculation for the rate and its derivatives, whereas scheme A and B are calculated straightforwardly using only the unstructured neighborhood information.

To show that the schemes are capable of solving more complex problems, an $\mathrm{n}^+\,\mathrm{p}\,\mathrm{n}\,\mathrm{n}^+$ structure was simulated in snap-back condition. Figure 5 shows the results of a quasi-static simulation, again all three schemes are depicted. In contrast to the diode example schemes A and B give slightly different results, the scheme of Laux is located in between A and B.

5. Conclusions

Two vector discretization schemes that are only based on the unstructured neighborhood information and that seamlessly integrate in the box integration method were presented. Both schemes allow to be used on Delaunay meshes, so orthogonal as well as triangular meshes can be used. The general formulation allows them to be used in 1D, 2D and 3D. Two examples were given, showing that these schemes can handle numerically challenging configurations very well and a comparison with the element based scheme from Laux was given. The different results show that a proper selection of the vector discretization method is important.

References

[1] SELBERHERR S., *Analysis and Simulation of Semiconductor Devices*, Wien–New York: Springer, 1984.

[2] KRAMER W. N. K., HITCHON G., *Semiconductor Devices, a Simulation Approach*, Prentice Hall Professional Technical Reference, 1997.

[3] SCHARFETTER D., GUMMEL H., *Large-Signal Analysis of a Silicon Read Diode Oscillator*, IEEE Trans. Electron Devices, vol. **16**, no. 1, pp. 64–77, 1969.

[4] LAUX S., GROSSMAN B., *A General Control-Volume Formulation for Modeling Impact Ionization in Semiconductor Transport*, IEEE Trans. Electron Devices, vol. **32**, no. 10, pp. 2076–2082, 1985.

[5] FISCHER C., *Bauelementsimulation in einer computergestützten Entwurfsumgebung*, Dissertation, Technische Universität Wien, 1994. [Online]. Available: `http://www.iue.tuwien.ac.at/phd/fischer/`

[6] IμE, *MINIMOS-NT 2.1 User's Guide*, Institut für Mikroelektronik, Technische Universität Wien, Austria, 2004. [Online]. Available: `http://www.iue.tuwien.ac.at/software/minimos-nt`